Environmental Science Nano

Emerging investigator series: Examination of the gastrointestinal lipidome of largemouth bass exposed to dietary single-walled carbon nanotubes.

Journal:	*Environmental Science: Nano*
Manuscript ID	EN-ART-04-2021-000303.R1
Article Type:	Paper

Environmental Significance Statement

Single Walled Carbon Nanotubes (SWCNTs) have a strong potential for environmental release due to their use in industrial and consumer products. These hydrophobic nanomaterials are likely to partition to sediments and biota, making diet a likely exposure route in fish. The gastrointestinal (GI) system serves a crucial role in the absorption of nutrients and lipids play an important part in the structure and functions of the GI. This study examines how SWCNTs alter the composition of lipids in the GI system. Results from this study will further our understanding of the potential environmental impacts of SWCNTs, even when these materials are not directly absorbed into aquatic organisms which is crucial for developing environmental policies for nanomaterials.

Title: Emerging investigator series: Examination of the gastrointestinal lipidome of largemouth bass exposed to dietary single-walled carbon nanotubes.

Alexis M. Wormington[1,2], Sarah E. Robinson[1,2], David Gabrielli[1,2], Mohammad-Zaman Nouri[2], Eric S. Coker[1], Nancy Denslow[2,3], Tara Sabo-Atwood[1,2], Joseph H. Bisesi Jr.[1,2*]

[1]Department of Environmental and Global Health, University of Florida, Gainesville, FL 32611

[2] Center for Environmental and Human Toxicology, University of Florida, Gainesville, FL 32611

[3]Department of Physiological Sciences, University of Florida, Gainesville, FL 32611

*Corresponding Author

Abstract

Carbon nanomaterials are emerging contaminants released into the environment primarily through anthropogenic processes, where they primarily partition into soils and sediments. Aquatic animals that inhabit, forage, or choose prey in the benthic zone are vulnerable to dietary exposure to sediment-associated carbon nanomaterials. Since carbon nanomaterials are hydrophobic, dietary exposure may alter the availability, metabolism, storage, and transport of lipids in the intestinal lumen or at the epithelial barrier, affecting downstream biological processes. To assess the effect of single-walled carbon nanotubes (SWCNTs) on the gastrointestinal lipidome of aquatic species, a feeding experiment with adult largemouth bass (*Micropterus salmoides*) was conducted. After 8 weeks of exposure to SWCNTs via the diet, the intestinal abundance of ceramides and several classes of lyso- and phospholipids were significantly altered. Additionally, functional profiling with Metaboanalyst revealed changes in pathways related to fatty acid biosynthesis in exposed fish. These results suggest that though SWCNTs do not pass through the gastrointestinal epithelium, they may alter gut homeostasis through interactions with intestinal lipids.

Introduction

Carbon nanomaterials are organic compounds that have seen increasing use in numerous commercial, industrial, and even medicinal applications[1,2]. Carbon nanomaterials come in several shapes, including tubes (e.g. single, double, and multi-walled) and spheres (e.g. fullerenes). The shape, structure, and functionalization of carbon nanomaterials convey different physical, electrical, and chemical properties allowing for diverse applications across several industrial and commercial fields. As their wholly carbonaceous composition makes carbon nanomaterials difficult to quantify in the environment, “cradle-to-grave” life cycle modeling has been utilized to estimate the burden of these compounds in the environment. Mueller and Nowak[3] predicted that 0.0003 tons (272 grams) of carbon nanotubes will be deposited into the water per year, and the predicted environmental concentration of carbon nanotubes in the United States and Europe was 0.001 and 0.004 ng/L in surface water and 14.8 and 8.6 ng/L in sewage treatment plant effluent, respectively[4]. Carbon nanotube levels in sediments were predicted to increase from 0.2 to 0.5 ug/kg between 2008 and 2012[4], matching the increase in carbon nanotube market value during that time period. As the demand for SWCNTs is still rising, there remains a need to assess the current environmental burden of SWCNTs. Like other carbon nanomaterials, SWCNTs are predicted to partition into the organic layers of soil and sediments following deposition from air or water[5]. Particularly in aquatic ecosystems, SWCNTs may enter the food chain when sediments are disturbed through physical disruptions or the activities of benthic inhabitants. For example, in a mesocosm experiment SWCNTs partitioned to sediment rapidly; however, after 10 months, SWCNTs were still found in the intestines of mosquitofish[5].

Multiple studies indicate that SWCNTs exhibit little acute toxicity in vertebrates[6,7] although several studies have reported sub-acute effects in fish and mammals[8–11]. In aquatic ecosystems, exposure likely occurs via the diet as low water solubility increases the ability of SWCNTs to adsorb to sediments and other particulates, thereby reducing the likelihood of a waterborne exposure. Though a dietary exposure to SWCNTs is possible, previous research from our group has shown that SWCNTs do not pass through the intestinal epithelium to enter circulation[12,13]. However, they can modulate the expression of protein transporters and other genes related to nutrient uptake in the gastrointestinal system[13]. Though SWCNT dietary studies in aquatic species are lacking, work conducted in rainbow trout (*Oncorhynchus mykiss*) suggests lipid peroxidation can occur in the brains of fish exposed to dietary SWCNTs[11].

The gastrointestinal epithelium is the first point of contact following a dietary exposure to a toxicant. As the site where nutrients are taken up, disruption of the lipid-rich epithelium may have detrimental impacts on an organism's ability to take up, package, and utilize essential nutrients, which could lead to deleterious effects on growth[14]. Additionally, as membranes are primarily comprised of lipids, they are especially vulnerable to the effects of nonpolar chemicals[15]. Due to their large surface area and lipophilic nature, SWCNTs may interact with numerous components of the gastrointestinal system, including nutrients, bile acids, epithelial membranes, and intestinal microbiota[9,13]. Indeed, chemicals sorbed to the surface of SWCNTs become bioavailable to the organism following oral exposure[16], suggesting these nanomaterials may preferentially interact with lipophilic biomolecules in the intestinal lumen or

epithelium. However, no analysis of global lipidomic disruption following oral exposure to SWCNTs has been conducted to-date.

The growing use of 'OMICS technology in the field of ecotoxicology has led to robust characterization of targeted and global biomolecular profiles in animals responding to environmental stressors[17,18]. Now more than ever, molecular mechanisms of toxicity are being explored using not only DNA but RNA, proteins, and metabolites. Metabolomics, including the emerging field of lipidomics, offers a method of assessing toxicity beyond the cellular level and provides insight into the organismal impact of environmental stressors, as metabolites are closely related to physiology[15,17]. Lipids are involved especially in cellular integrity, signaling, and energy storage and may provide valuable information regarding the impact of toxicants that preferentially interact with nonpolar molecular targets. Though biologically ubiquitous, lipids are concentrated in some tissues more than in others, particularly in the gastrointestinal system and in secretary organs (e.g. gonads, liver, brain)[19,20]. Thus, lipidomics analyses may help answer more specific questions regarding the function of lipid-heavy systems following exposure to an organic chemical, such as SWCNTs.

In this study, a semi-quantitative lipidomics approach was utilized to explore the gastrointestinal toxicity of dietary SWCNTs in largemouth bass (LMB, *Micropterus salmoides*), an alternative predatory model. LMB are one of the most popular freshwater game fish in North America and are widespread, especially in the southern United States. As top-tier predators adaptive to waters of different hydrodynamic characteristics, such as lakes, ponds, and rivers, LMB prey on organisms from a variety of ecological niches and may be exposed to SWCNTs directly through benthic interactions or by consumption

of exposed prey. Additionally, LMB grow to a large size, with growth influencing individual fitness and reproductive success during seasonal spawning[21], placing an emphasis on efficient energy utilization and storage in these fish. The tight energy budget of predatory fish makes LMB an ideal model for dietary exposure to a chemical potentially affecting intestinal homeostasis and nutrient uptake.

Experimental

Animals and Housing

All experiments were conducted in accordance to The Guide for the Care and Use of Laboratory Animals under the supervision of the University Florida Institutional Animal Care and Use Committee. LMB fingerlings were sourced from the Florida Bass Conservation Center in Webster, FL and housed in outdoor 250-gallon tanks at the Aquatic Toxicology Core Laboratory at the University of Florida. Tanks were maintained as flow through systems with dechlorinated tap water from the City of Gainesville, and water temperatures were allowed to fluctuate seasonally (12.8-28°C) to maintain proper reproductive function for this synchronous spawning species. Fish were fed pelletized slow-sinking fish feed (5 mm; Skretting, USA) daily and reared until sexual maturity (approximately 1-2 years old).

SWCNT Characterization and Food Preparation

SG56 SWCNTs (Sigma-Aldrich, USA) were suspended in a solution of 0.5% acacia gum arabic (Sigma Aldrich, USA) in Milli-Q water by probe sonication (Branson, USA) at 1 mg/mL, following a method for suspension preparation that leads to highly repeatable particle characteristics that have been reported in our previous manuscripts[12,13,16]. Microtip probe settings were as follows: 8 seconds on and 2 seconds off at 50% amplitude

for 10 minutes followed by 10 minutes at 30% amplitude. Suspension was centrifuged at 14000 rpm for 20 minutes and re-sonicated for 10 minutes at 30% amplitude. Characterization of these suspensions has previously been reported in Bisesi et al., 2014[12] which showed an average aggregate size of 132 nm, moderately compact aggregates with a fractal dimension of 2.2–2.3, and <5% w/w metal catalyst with ~3.8% molybdenum and ~0.93% cobalt leaching from these materials when suspended. According to the manufacturer, the average SWCNT diameter was 0.78 nm and the median tube length was 1 μm. As a result, these materials have a high aspect ratio (>1000) with a surface area of ≥700 m^2/g. Previous characterization data indicates that these suspensions are stable for at least a week, and suspensions were prepared 24 hours prior to making the food.

Due to the fluorescence of SG65 nanoparticles at near-infrared wavelengths, near-infrared fluorescence (NIRF) was utilized to quantify the SWCNT suspension. SG65 SWCNTs have inherent fluorescence properties that are highly dependent on aggregation state. NIRF was used to characterize suspensions in this study as NIRF is sensitive to poorly suspended materials and alterations in particle aggregation. Numerous studies have demonstrated the utility of this approach for these specific nanomaterials in the characterization of SWCNT suspensions as well as SWCNTs associated with biological tissues [5,12,22–28] NIRF Excitation of samples was achieved with a BWF1 high brightness fiber coupled laser system (450 mW; BW Tech, USA). Emission was measured using a liquid nitrogen cooled Princeton Instruments OMA V InGaAs one-dimensional array detector (1024x1 pixels) coupled with an Acton SP2300 spectrograph controlled by WinSpec Software (Princeton Instruments, Trenton, NJ). Samples were measured in a

glass cuvette that allows for perpendicular excitation by the laser and emission measurement in the system described above. Samples were excited with the laser for 5 seconds followed by measurement of emission spectra from 750 to 1500 nm. A SWCNT standard curve was created in 2% sodium deoxycholate (SDC, Thermo Fisher Scientific, USA), a surfactant that has been shown to produce homogenous disaggregate suspensions of nanotubes. The gum arabic/SWCNT suspension was diluted by 100 in 2% SDC before a NIRF reading was recorded (peak emission, ~986 nm). Approximate concentration of the original suspension was calculated from the standard curve (r^2 = 0.99, y = 1E+06x + 1452.7).

Concentrated suspensions described above were diluted in 100 ml containing 0.5% gum arabic, 0.3% triethylene glycol, and 0.7% methanol to reach the final SWCNT concentration. Our target concentration was 0.025 mg/mL (which would have equal 2.5 mg/kg food), but when the SWCNT solution was assessed via NIRF, our nominal concentration was found to be 0.017 mg/mL (i.e. 1.7 mg/kg food). Previous experiments with SG65 SWCNTs utilized a dose of 2.5 mg/L for fate studies in wetlands[5]; therefore we wanted to use a similar dose in feeding experiments (2.5 mg/kg). Additionally, Bisesi et al. 2017[16] utilized a 25 µg SWCNT single gavage dose. For this experiment, we chose to use a SWCNT dose that was an order of magnitude less than 2.5 µg/fish/day because the fish were being exposed for a longer period of time (2 months).

This solution was added to 1 kg pelletized 3.0 mm salmon sink (Skretting, USA) over two hours (25 mL every 30 mins) in a KitchenAid Stand Mixer. Control feed was prepared in the same manner without the addition of SWCNTs. Both feeds were transferred to a cold

room (4°C) and coated in 100 mL gelatin while continuing mixing (four 25 mL batches added over 2 hours). Food was stored at -20°C until use.

Exposure

Adult largemouth bass were taken from our established culture and dorsally tagged with passive integrated transponders (PIT) for identification. Mass and fork length was recorded before fish were distributed into two 150-gallon indoor round tanks. Indoor water temperatures fluctuated between 23.1 and 28.2°C during the experimental period. The exposure included two tanks with 18 fish each. Nets were placed over the top of the tanks to prevent fish from jumping out; however, 1 fish was lost due to jumping in the SWCNT-Fed tank (17 fish at the end of the experiment for this tank).

Fish were acclimated to experimental aquaria for at least one month and re-weighed prior to exposure. Experimental animals were 138 ± 37 grams on average for controls and 121 ± 30 grams on average for SWCNT-Fed. There was no significant difference in growth between the two treatment groups, with controls and SWCNT-Fed fish growing 4 ± 2% and 7 ± 5% on average compared to their initial weight. Fish were fed daily to satiation throughout the acclimation and experimental periods, and animals were fasted for 24 hours before the first feeding of control and SWNT-coated food. Feeding amounts were approximately quantified with measuring cups and recorded. Tanks received between 0.5 and 1.25 scoops of food per day (1 scoop = 18.2 grams). There was a slight increase in mean daily food intake (g food per fish) in the SWCNT-Fed tank. This did not translate to a treatment-related impact on growth, likely because the difference in mean food intake,

though significant, was very small (0.89 ± 0.27 vs 0.93 ± 0.18 g food/fish/day in controls and SWCNT-Fed fish, respectively).

Dietary exposure occurred for 8 weeks. Stress behaviors, such as flashing, disrupted equilibrium, or antisocial behavior, were not observed at any point during the experiment. After the exposure, fish were euthanized with MS-222 and necropsied. Tissues were flash-frozen in liquid nitrogen and stored at -80°C until analysis.

Lipidomics

The Bligh and Dyer method[29] was utilized to extract and purify total lipids from gut and liver tissue. 30 mg gut (10 mg each of proximal, middle, and distal sections; pooled) was homogenized with a T-10 Basic ULTRA-TURRAX® disperser (IKA Works Inc., USA) in 1 mL LC-MS grade water. 30 mg liver was processed similarly. Samples were placed on ice for 10 minutes, and lipids were extracted in a solution of 2 mL methanol and 0.9 mL dichloromethane (DCM). After vortexing, samples were spiked with 50 µL EquiSPLASH LIPIDOMIX analytical standard (Avanti Polar Lipids, USA, Supplementary Table 2), diluted 1 to 5 in methanol before adding to the samples. Following a 30-minute incubation at room temperature, samples received 1 mL LC-MS grade water and 0.9 mL DCM. Tubes were then inverted and centrifuged at 1200 rpm for 10 minutes. The bottom layer was transferred to an autosampler vial and dried under nitrogen gas. Samples were re-extracted in 2 mL DCM and centrifuged. The bottom layer was collected, combined with the first extract, and dried under nitrogen gas. Extracts were reconstituted in ethanol.

A QTrap 6500 Linear Ion Trap Quadrupole LC/MS/MS (AB SCIEX, Canada) instrument was used to identify and quantify lipids. Mobile phases A and B were 95:5

acetonitrile:water and 50:50 acetonitrile:water, respectively, both with 1mM ammonium acetate. The pH of both mobile phases was adjusted to 8.2. Mobile phase B increased to 6% in 6 minutes, to 25% in 10 minutes, to 98% in 11 minutes, and then to 100% in 13 minutes. Separation was conducted with Shimadzu Nexera X2 LC system (Shimadzu Corporation, Japan) and an XBridge Amide column (3.5 µm, 4.6x150 mm; Waters, Ireland). The scan type was multiple reaction monitoring in both positive and negative ion mode, conducted with Analyst® Software. Relative abundance for each lipid was quantified in MultiQuant Software using the integrated peak area of the EquiSPLASH standard closest in structure. Scan information for all lipids is included in Supplementary Tables 3 and 4. The data obtained in this study will be accessible at the NIH Common Fund's NMDR (supported by NIH grant, U01-DK097430) website, the Metabolomics Workbench, https://www.metabolomicsworkbench.org.

Statistical Analysis

Data were analyzed in R (R Studio, Boston, MA, USA), Primer 7 (Primer-e, Albany, Auckland, New Zealand), and GraphPad Prism 8 (GraphPad Software Inc, La Jolla, CA, USA). Missing values below the limit of detection were imputed using half the minimum value for the missing lipid, a common and consistent imputation method for LC-MS data[30]. Lipid classes and individual lipid species were normalized by percent of total lipid (lipid class or species divided by sum of total lipids). Class level data was tested for departure from normality using Shapiro-Wilks test in Prism 8. Individual lipids were compared using Wilcoxon Rank Sum tests in R, class level lipids were compared by either t-tests (parametric) or Wilcoxon Rank Sum tests (nonparametric) in Prism 8. To account for multiple comparison statistical tests, the false discovery rate adjustment was applied to a

vector of *p*-values in R. Non-metric multidimensional scale (NMDS) analyses followed by permutational multivariate analysis of variance (PERMANOVA) were run on individual level and class level lipid data using Primer 7. A list of *p*-values for significant lipid species are included in Supplementary Table 1.

A limited pathway analysis was conducted for the gut data using MetaboAnalyst. ID numbers from the Human Metabolome Database (HMDB IDs) were obtained for the identified lipid species. Out of 869 lipids, 548 had HMDB IDs (63%). Individual TAGs with the same fatty acid composition had the same HMDB ID and were summed (439 TAGs into 21 HMDB ID categories). Of the 179 individual or summed lipids input into MetaboAnalyst, 126 had associated KEGG IDs from which pathways could be predicted. The zebrafish (*Danio rerio*) lipidome was selected as a reference. The "Globaltest" pathway enrichment method was selected, and the node importance measure chosen for topological analysis was "relative betweenness centrality".

Results & Discussion

As a major component of cells and cell membranes, lipids serve not only as important biomarkers of structural disruption but may indicate alterations in signaling related to various gastrointestinal activities. The objective of this study was to determine how dietary exposure to SWCNTs may affect the gastrointestinal lipidome of largemouth bass. EquiSPLASH LIPIDOMIX was utilized to identify and quantify ~870 lipids across 18 different structural classes, including sphingolipids, phospholipids, and glycerolipids in LMB exposed to foodborne SWCNTs for 8 weeks.

Though lipids in the gut and liver were quantified, treatment-related changes were primarily identified in the gut (Figure 1B, Supplementary Table 1), with minimal impact on

the liver. These results are in line with previous work from our group showing the inability of SWCNTs to cross the intestinal epithelium[12]. A non-metric dimensional scaling (NMDS) analysis was used to assess statistical relationships between treatments at both the lipid class and species levels for gut and liver samples. In the gut, at the level of lipid class, control and treated fish were similar in compositional abundance; however, NMDS analyses at the level of lipid class were limited by the semi-quantitative approach, as some classes were much higher in abundance (e.g. TAGs, PEs) simply due to more lipids in that class being identified. NMDS analyses between treatments at the level of lipid species showed significant dissimilarity (PERMANOVA p=0.003, Figure 1B). To elucidate interactions at the level of lipid species, FDR-corrected Wilcoxon rank-sum tests were used to compare the treatments. Out of 869 identified lipid species spanning 18 different classes, 81 lipids were significantly altered (FDR-adjusted p<0.05) in the guts of treated fish (Figure 2B). One lipid, TAG(51:0/FA17:0), was altered in the liver. Impacted gut and liver lipids and their FDR-adjusted p-values are reported in Supplementary Table 1. Gut lipid classes with numerous species affected by the SWCNT diet were the hydoxyceramides (HCERs), lysophosphatidylethanolamines (LPEs), lysophosphatidylglycerols (LPGs), phosphatidylcholines (PCs), and phosphatidylserines (PSs), with a 20-50% alteration in lipids from these classes (Figure 2B).

Additionally, gut and liver lipids were analyzed by sex for both treatment groups. PERMANOVA analysis of global lipidomes indicated that were was not a statistically significant difference between males and females in the gut; however, there was a difference between sexes in the liver (PERMANOVA p=0.02). Exploration of the liver data at the lipid class level revealed a significant Kruskal-Wallis test by sex for several classes,

but this was not reflected in multiple comparisons testing. Lastly, of gut lipids at the class level indicated that the only sex specific differences were in the cholesterol esters between control males and control females.

Of the significantly affected lysophospholipids outlined in Figure 3, two LPG and one LPC species increased in the SWCNT treatment group (LPGs 20:1 and 20:2; LPC 22:5). LPEs were the most impacted by the treatment, with eight out of sixteen detected LPE species decreased in the guts of SWCNT-Fed fish (LPEs 22:4, 22:5, 16:0, 16:1, 18:1, 18:2, 18:3, and 20:0, Figure 3C). Lysophospholipids are generated through phospholipase action on precursor phospholipids. Though lysophospholipids are in low abundance compared to other phospholipids, evidence suggests that they are strong lipid signals and act through G-coupled protein receptors[31], namely in immunoreactive pathways. LPCs, LPGs, and LPEs are understudied and *in vivo* physiological information is limited, especially in fish. LPCs, formed from PCs and cholesterol and involved in the same biosynthetic pathway as cholesterol esters[32], are potent promotors of lipid uptake and secretion of intestinal alkaline phosphatase, an anti-inflammatory enzyme, *in vitro*[33,34]. LPGs stimulate chemotactic migration in human immune cells[35] and are generally anti-inflammatory[36]. LPEs may play a role in gut homeostasis as oral administration of LPEs have been associated with reduced epithelial integrity and disease-status in mice[37]. In our study, LPCs and LPGs were reduced in SWCNT-Fed fish (Figure 3A & 3B), while LPEs were increased (Figure 3C). The differential abundance of these lysophospholipids may be attributed to their varying physiological roles in lipid uptake and inflammation. Compared to LPCs and LPGs, LPEs were more impacted by SWCNT treatment, and their elevation suggests a potential inflammatory response in the guts of SWCNT-Fed LMB.

Additionally, enrichment in gut phospholipids was observed, with nineteen PCs, seven PSs, two PGs, and two PEs increased in the guts of treated fish (Figure 4). PCs are a major component of cell membrane and are responsive to potent lipid signals such as ceramides, which can alter the physiochemical properties of PC lipid bilayers by activating membrane phospholipases[38] and impacting membrane assembly[39]. Other major membrane phospholipids are PSs, which under normal conditions are maintained asymmetrically in the membrane and act as a protective blockade in the intestinal epithelium[40]. Externalization of PSs is associated with disease and could be a sign of apoptosis[41]. Notably, SWCNT-exposed fish had elevated PC and PS levels in the gut, suggesting membrane toxicity in the intestinal epithelia, possibly related to membrane inflammation. Though none of the significantly changed PSs outlined in Figure 4 had associated HMDB IDs (Supplementary Table 1), limiting the scope of the functional analysis conducted in MetaboAnalyst (Table 1), dietary SWCNTs have been associated with inflammatory endpoints in other studies. Rainbow trout fed a diet containing SWCNTs had elevated thiobarbituric acid-reacting substances (TBARs) in the brain after 4 weeks of exposure[11]. Intravenous injection of SWCNTs resulted in increased spleen TBARs in rainbow trout[7]. Though TBAR elevation in the gut was not observed in either study, our results indicate a potential inflammatory response mediated by membrane phospholipids. Disrupted metabolites, including those measured in this study (i.e. palmitic acid and triglycerides) were biomarkers of intestinal inflammation in zebrafish exposed to microplastics[42], further highlighting the potential of metabolomics to identify sublethal impacts, such as inflammation, on the fish gastrointestinal system during dietary exposures. Intestinal inflammation can contribute to several negative outcomes (e.g.

microbial dysbiosis and increased epithelial permeability) with the potential to disrupt nutritional and metabolic state as well as growth in fish.

Among the sphingolipids, only the hydroxyceramides (HCERs) were altered by treatment, with seven HCERs decreased in the gut (HCERs 20:0, 20:1, 22:1, 24:0, 24:1, 26:0, and 26:1; Figure 5). Ceramides are primarily involved in cell signaling processes such as inflammation, membrane integrity, fatty acid metabolism, and apoptosis and are a precursor to the other major sphingolipids[43]. Bacteroides of the gut microbiome play a key role in the production of these sphingolipids, with decreases in *de novo* sphingolipid production associated with increased liver ceramide levels; however, the interaction between SWCNT and gut bacteria has not been investigated[44]. Significantly altered brain ceramide levels were found in the brains of schizophrenic and bipolar patients[45], further highlighting the signaling role of ceramides, especially in stress and inflammatory pathways. Specifically, HCERs, all decreased by SWCNT treatment, are more potent apoptotic signals than ceramides[46]. Lastly, ceramides are thought to be highly involved in insulin signaling and obesity due to their role in fatty acid metabolism, and decreases in ceramide levels have been associated with reduced fat deposition in rodent models[47].

Several triacylglycerides (TAGs) and one diacylglyceride (DAG) were also affected and primarily diminished in SWCNT-Fed fish (Figure 6). In fish, TAGs and DAGs are utilized for short-term energy storage until the fatty acids are mobilized during activity, such as migration[48]. Particularly, largemouth bass accumulate high amounts of TAGs, highlighting their importance for energy homeostasis in these large, predatory fish. The reduction in numerous gut TAGs in SWCNT-Fed fish could be indicative of decreased nutrient uptake.

Our findings coincide with previous experiments, in which genes related to nutrient transport were altered in the guts of fathead minnows exposed to dietary SWCNTs[13].

With many thousands of lipids spanning different compositions and subtypes, it can be difficult to relate lipidomic alterations to impacts on organs or individuals. In other 'OMICS disciplines, the gap between molecule and function has been addressed with predictive frameworks and databases, such as the Kyoto Encyclopedia of Genes and Genomes (KEGG). KEGG draws from large molecular datasets, including genome sequences and transcriptomic profiles, to make predictions about functions related to specific molecules, namely genes[49]; however, lately the utility of KEGG has been expanded to include functional characterization of metabolomic profiles through pathway analysis. Many metabolites have associated KEGG IDs, which can be input into pathway prediction software (e.g. PICRUSt, MetaboAnalyst) to draw conclusions about a specific dataset[50]. As functional lipidomics research is still in its infancy, many lipids do not have pathway identifiers. Almost 37% of the individual lipids in our dataset did not have identifiers from the Human Metabolome Database, namely the phospholipids, and several lipids had the same identifier (TAGs); however, even the partial pathway analysis of the gut lipidomics data in MetaboAnalyst was informative (Table 1). See Supplementary Table 1 for specific HMDB ID information for this dataset.

Of the two near-significantly affected pathways in MetaboAnalyst (FDR-adjusted $p \sim 0.05$), both were related to fatty acid biosynthesis and metabolism and were diminished in SWCNT-Fed fish. This could be a result of a reduction in TAGs and DAGs (Figure 6), which are a direct source of stored fatty acids. Within the fatty acid biosynthesis pathway identified in MetaboAnalyst, myristic acid (KEGG ID C00249) and palmitic acid (KEGG ID

C06424) were impacted. Both palmitic and myristic acid are involved in the *de novo* synthesis of ceramides—palmitic acid is metabolized into palmitoyl-CoA, the first metabolite in the ceramide synthesis pathway[51], and myristic acid is a potent activator of Dihydroceramide Δ4-desaturase 1, which catalyzes the final step of *de novo* ceramide biosynthesis[52]. Thus, the predicted effect on fatty acid signaling pathways in the guts of treated fish could be related not only to reduced DAG/TAG levels but to reduced HCER abundance in SWCNT-exposed fish (Figure 5). Only half of the HCERs had associated HMDB IDs (Supplementary Table 1), which may have reduced the power of the pathway analysis in MetaboAnalyst. However, the connection between hydroxyceramides, palmitic acid, and myristic acid as it relates to fat deposition and insulin signaling is notable. Palmitic acid, increased in SWCNT-Fed fish, may be involved in the inhibition of ceramide accumulation related to insulin signaling[53,54]. Palmitic acid is a long-chain fatty acid highly studied in the field of medicine due to its direct contributions to the development of cellular insulin-resistance in mammals[55,56]. Insulin functions differently in fish than in mammals—carnivorous fish do not utilize carbohydrates efficiently and are frequently glucose intolerant[57]. However, glucose intolerance in carnivorous fish is not modulated by insulin, as it is in mammals[58]. As fish insulin plays an essential role in growth through the promotion of lipogenesis and inhibition of lipolysis[59], cellular insulin resistance induced by elevated palmitic acid signaling could bear consequences for fish heavily reliant on the storage of visceral fat for successful reproduction[60] and the survival of prey-scarce winter seasons[61].

In conclusion, lipidomics analysis revealed that exposure to the SWCNTs changed the levels of important signaling lipids between the guts of control and treated fish. Though

SWCNTs do not pass through the intestinal epithelium, a hypothesis further validated by the lack of major effects observed in the liver, our data suggests foodborne SWCNTs may cause dietary toxicity to LMB, namely in the metabolism of fatty acids and abundance of ceramides, di- and triacylglycerols, lysophospholipids, and other lipid signals in the intestinal tract. Chronic exposure to SWCNTs could lead to inflammation as well as downstream effects on the metabolism and accumulation of fats essential for growth, especially in long-lived species, such as LMB. As LMB are known to live for over 20 years in the wild, deleterious impacts of chronic dietary exposure to SWCNTs may take longer periods to manifest. As the demand and use for these materials is predicted to increase in the coming years[62], additional research should (1) investigate exposure to non-pristine carbon nanomaterials, such as functionalized nanotubes, and (2) assess the impact of nanomaterials over longer exposures than the 8 weeks used in this study in order to better replicate a realistic exposure scenario and understand the potential long-term impact of foodborne SWCNTs on lipids.

Acknowledgements

The authors have no conflict of interest to disclose. This work was funded by a grant from the National Science Foundation (CBET Award Number 1605119, to JHB and TSA).

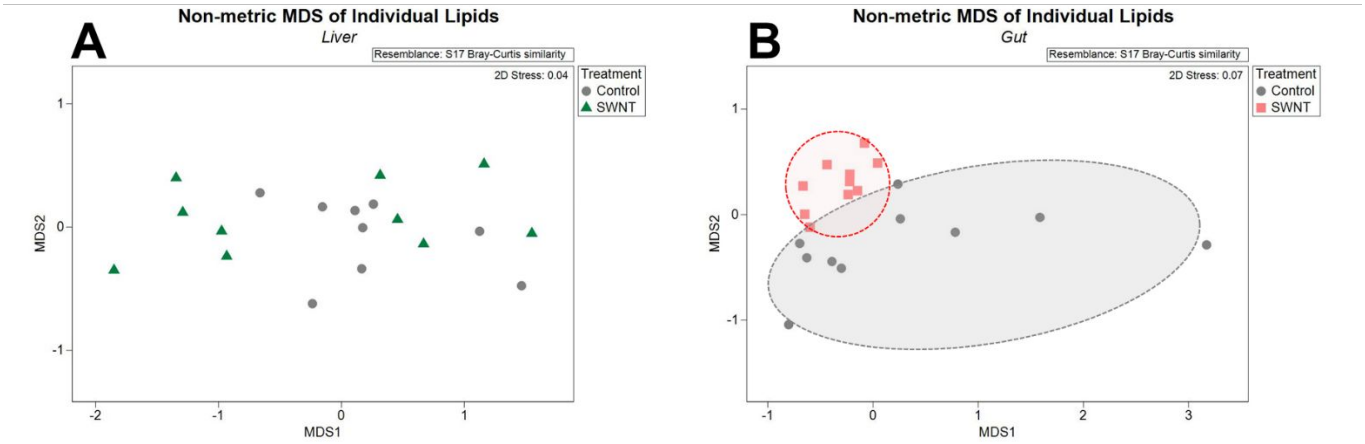

Figure 1: Non-metric multidimensional scaling (NMDS) plots of global lipid profiles by treatment group. Individual lipid abundances were normalized by percent of total lipid abundance for each fish. A) NMDS for liver lipids. Permutational ANOVA not significant. B) NMDS for intestinal lipids. Permutational ANOVA p=0.003.

A

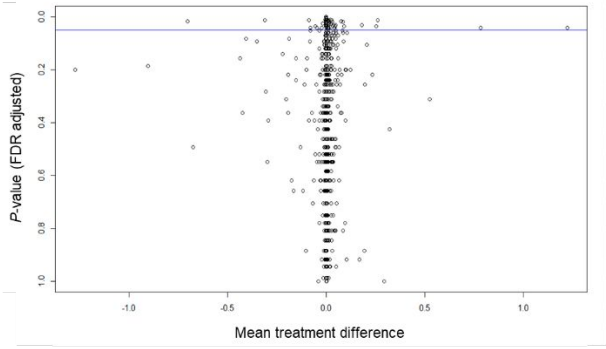

B

Lipid Class	Significantly Impacted (p<0.05)	Total Measured	% Affected
Cholesterol Esters (CE)	0	12	0
Ceramides (CER)	0	12	0
Dihydroceramides (DCER)	0	11	0
Hydroxyceramides (HCER)	7	11	63.6
Lactosylceramides (LCER)	0	1	0
Diacylglycerol (DAG)	1	31	3.2
Lysophosphatidylcholine (LPC)	1	16	6.3
Lysophosphatidylethanolamine (LPE)	8	16	50
Lysylphosphatidylglycerol (LPG)	2	10	20
Lysophosphatidylinositol (LPI)	0	3	0
Lysophosphatidylserine (LPS)	0	1	0
Monoacylglycerol (MAG)	0	6	0
Phosphatidylcholine (PC)	19	50	38
Phosphatidylethanolamine (PE)	5	125	4
Phosphatidylglycerol (PG)	2	64	3.1
Phosphatidylinositol (PI)	0	60	0
Phosphatidylserine (PS)	7	19	36.8
Sphingomyelin (SM)	0	12	0
Triacylglyceride (TAG)	29	409	7.09
Total	81	869	

Figure 2: Results of significance testing of individual gut lipids between control and SWCNT-Fed fish. A: Volcano plot displaying significance level (FDR p-value) against difference in percent of total abundance between treatments. Lipids above the blue line are significantly changed (FDR p<0.05). B: Table detailing the significantly affected lipid species by lipid class.

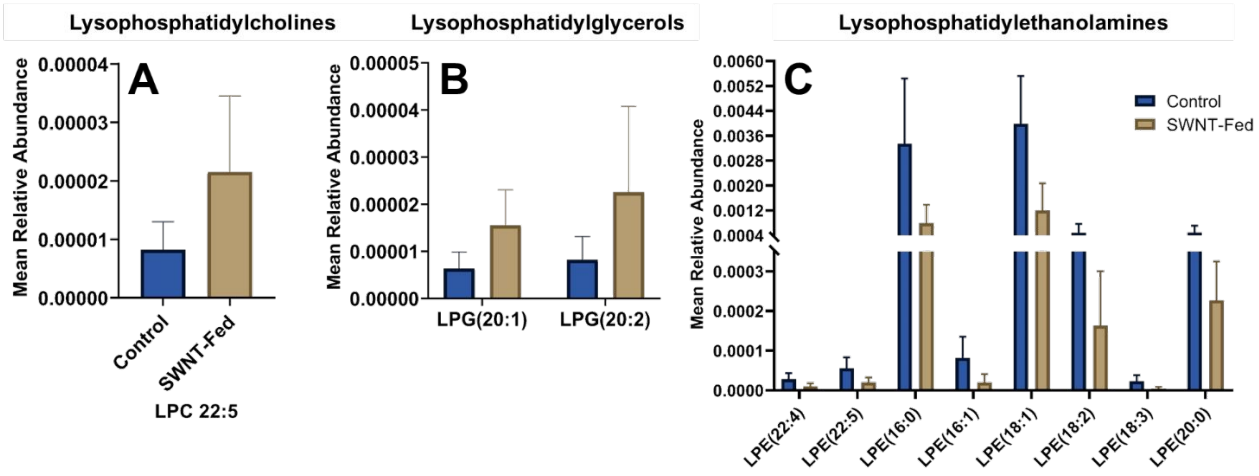

Figure 3: Gut lysophospholipids (A: lysophosphatidylcholines, B: lysophosphatidylglycerols, C: lysophosphatidylethanolamines) significantly altered (FDR p<0.05) in SWCNT-Fed fish compared to controls.

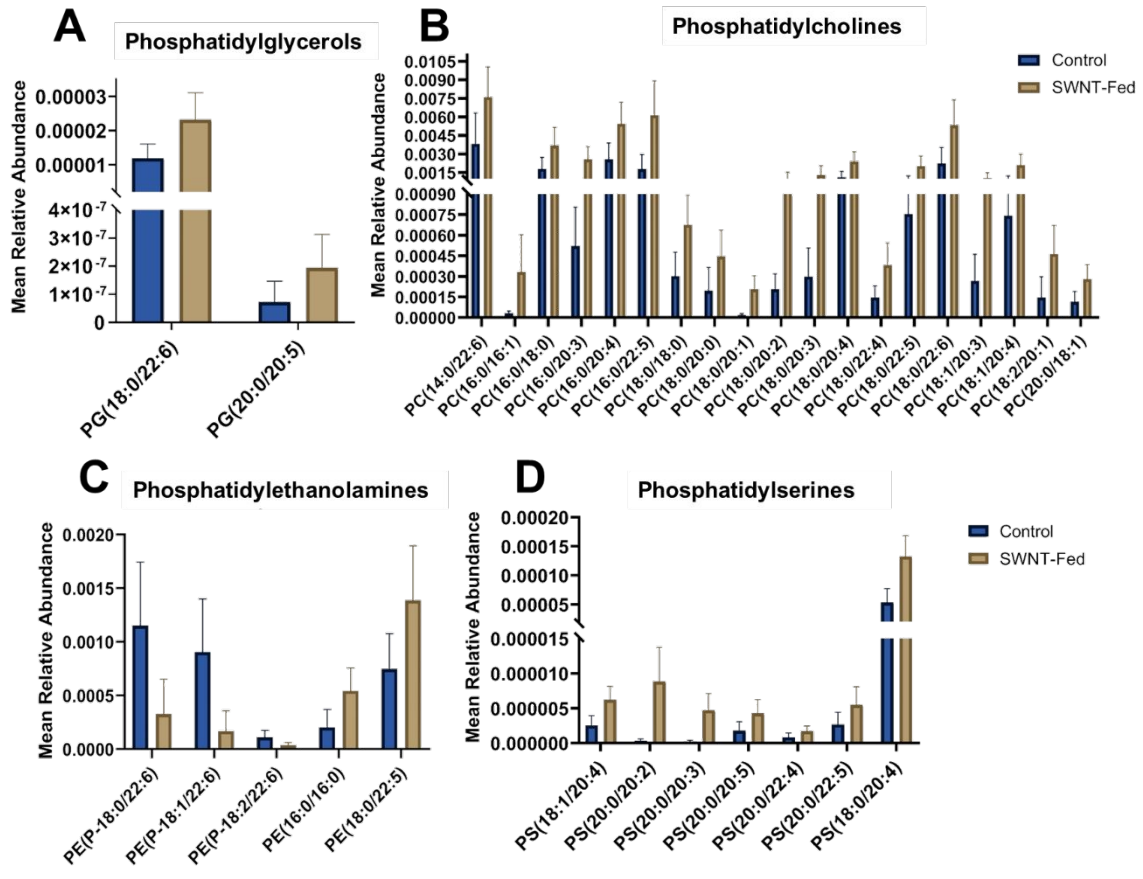

Figure 4: Gut phospholipids (A: phosphatidylglycerols, B: phosphatidylcholines, C: phosphatidylethanolamines, D: phosphatidylserine) significantly altered (FDR p<0.05) in SWCNT-Fed fish compared to controls.

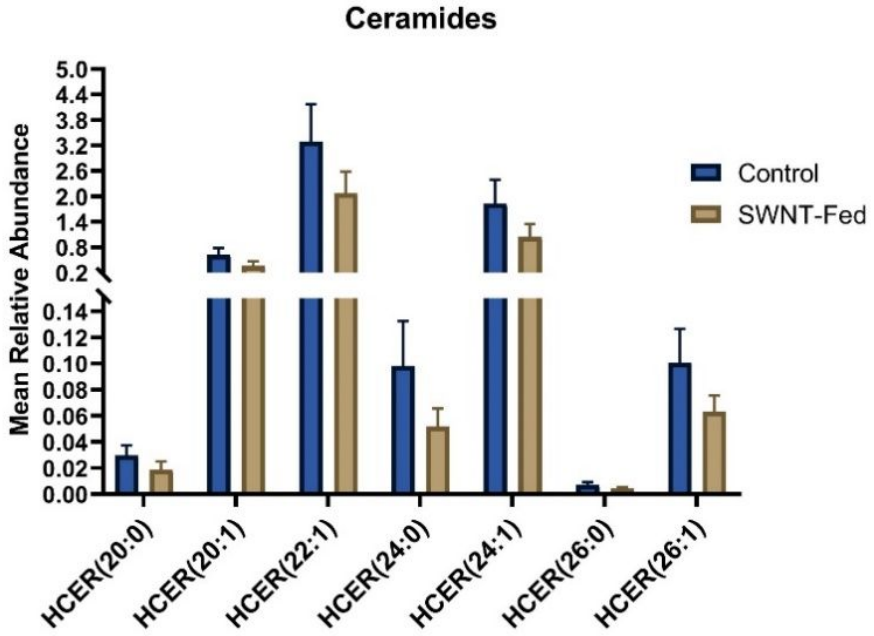

Figure 5: Gut hydroxyceramides significantly altered (FDR p<0.05) in SWCNT-Fed fish compared to controls.

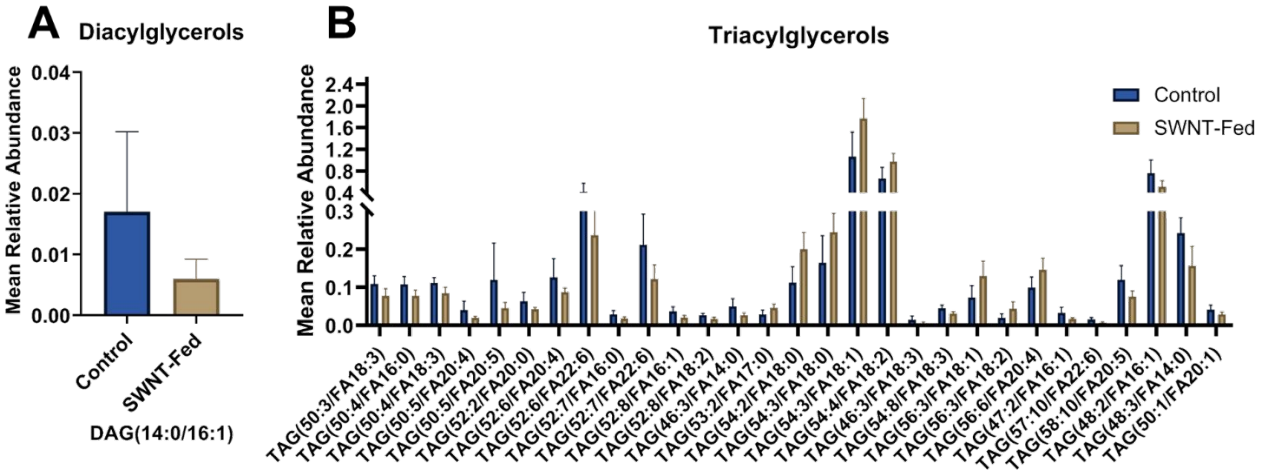

Figure 6: Gut diacylglycerides (A) and triacylglycerides (B) significantly altered (FDR p<0.05) in SWCNT-Fed fish compared to controls.

Table 1: MetaboAnalyst-generated pathway enrichment and topology analysis of a subset of the lipid abundance data compared to a reference lipidome (*Danio rerio*).

			Pathway Enrichment		Pathway Topology
Pathway	Total Computed	Hits	Raw p	FDR p	Impact
Fatty acid biosynthesis	47	2	0.008	0.055	0.015

Biosynthesis of unsaturated fatty acids	35	10	0.01	0.055	0
Steroid biosynthesis	42	1	0.027	0.098	0
Fatty acid elongation	39	1	0.08	0.149	0
Fatty acid degradation	38	1	0.08	0.149	0
Sphingolipid metabolism	21	3	0.081	0.149	0.308
Arachidonic acid metabolism	33	2	0.172	0.27	0.311
Linoleic acid metabolism	4	2	0.196	0.27	1
alpha-Linolenic acid metabolism	13	2	0.261	0.319	0.333
Glycerophospholipid metabolism	38	3	0.324	0.356	0.202
Glycosylphosphatidylinositol (GPI)-anchor biosynthesis	13	1	0.658	0.658	0.005

References

1 K. P. Loh, D. Ho, G. N. C. Chiu, D. T. Leong, G. Pastorin and E. K.-H. Chow, *Adv. Mater.*, 2018, **30**, 1802368.

2 T. Chen and L. Dai, *Mater. Today*, 2013, 16, 272–280.

3 N. C. Mueller and B. Nowack, *Environ. Sci. Technol.*, 2008, **42**, 4447–4453.

4 F. Gottschalk, T. Sonderer, R. W. Scholz and B. Nowack, *Environ. Sci. Technol.*, 2009, **43**, 9216–9222.

5 A. Schierz, B. Espinasse, M. R. Wiesner, J. H. Bisesi, T. Sabo-Attwood, P. Lee Ferguson, P. L. Ferguson and P. Lee Ferguson, *Environ. Sci. Nano*, 2014, **1**, 574–583.

6 S. T. Yang, X. Wang, G. Jia, Y. Gu, T. Wang, H. Nie, C. Ge, H. Wang and Y. Liu, *Toxicol. Lett.*, 2008, **181**, 182–189.

7 D. Boyle, P. A. Sutton, R. D. Handy and T. B. Henry, *Environ. Pollut.*, 2018, **232**,

191–199.

8 C. A. Poland, R. Duffin, I. Kinloch, A. Maynard, W. A. H. Wallace, A. Seaton, V. Stone, S. Brown, W. Macnee and K. Donaldson, , DOI:10.1038/nnano.2008.111.

9 H. Chen, R. Zhao, B. Wang, L. Zheng, H. Ouyang, H. Wang, X. Zhou, D. Zhang, Z. Chai, Y. Zhao and W. Feng, *Adv. Healthc. Mater.*, 2018, **7**, 1701313.

10 C. J. Smith, B. J. Shaw and R. D. Handy, *Aquat. Toxicol.*, 2007, **82**, 94–109.

11 T. W. K. Fraser, H. C. Reinardy, B. J. Shaw, T. B. Henry and R. D. Handy, *Nanotoxicology*, 2011, **5**, 98–108.

12 J. H. Bisesi, J. Merten, K. Liu, A. N. Parks, A. R. M. N. Afrooz, J. B. Glenn, S. J. Klaine, A. S. Kane, N. B. Saleh, P. L. Ferguson and T. Sabo-Attwood, *Environ. Sci. Technol.*, 2014, **48**, 1973–1983.

13 J. Bisesi, T. Ngo, S. Ponnavolu, K. Liu, C. Lavelle, A. R. M. Afrooz, N. Saleh, P. Ferguson, N. Denslow and T. Sabo-Attwood, *Nanomaterials*, 2015, **5**, 1066–1086.

14 A. Abdel-moneim, M. Moreira-Santos and R. Ribeiro, *Chemosphere*, 2015, **120**, 568–574.

15 D. A. Dreier, J. A. Bowden, J. J. Aristizabal-Henao, N. D. Denslow and C. J. Martyniuk, *Comp. Biochem. Physiol. - Part D Genomics Proteomics*, 2020, **36**, 100742.

16 J. H. Bisesi, S. E. Robinson, C. M. Lavelle, T. Ngo, B. Castillo, H. Crosby, K. Liu, D. Das, J. Plazas-Tuttle, N. B. Saleh, P. L. Ferguson, N. D. Denslow and T. Sabo-Attwood, *Environ. Sci. Technol.*, 2017, **51**, 948–957.

17 P. A. Bahamonde, A. Feswick, M. A. Isaacs, K. R. Munkittrick and C. J. Martyniuk, *Environ. Toxicol. Chem.*, 2016, **35**, 20–35.

18 X. Zhang, P. Xia, P. Wang, J. Yang and D. J. Baird, *Environ. Sci. Technol.*, 2018, **52**, 3842–3851.

19 M. A. Sheridan, *Comp. Biochem. Physiol. -- Part B Biochem.*, 1988, 90, 679–690.

20 S. A. Murzina, C. A. Meyer Ottesen, S. Falk-Petersen, H. Hop, N. N. Nemova and O. G. Poluektova, *Fish Physiol. Biochem.*, 2012, **38**, 1393–1407.

21 J. W. Neal and R. L. Noble, *Trans. Am. Fish. Soc.*, 2006, **135**, 1535–1545.

22 J. Nicholas, H. Chen, K. Liu, I. Venu, D. Bolser, N. B. Saleh, J. H. Bisesi, W. Castleman, P. L. Ferguson and T. Sabo-Attwood, *NanoImpact*, 2019, **14**, 100167.

23 A. Schierz, A. N. Parks, K. M. Washburn, G. T. Chandler and P. L. Ferguson, *Environ. Sci. Technol.*, 2012, **46**, 12262–12271.

24 A. N. Parks, L. M. Portis, P. A. Schierz, K. M. Washburn, M. M. Perron, R. M. Burgess, K. T. Ho, G. T. Chandler and P. L. Ferguson, *Environ. Toxicol. Chem.*, 2013, **32**, 1270–1277.

25 H. Hong, T. Gao and W. Cai, *Nano Today*, 2009, 4, 252–261.

26 M. D. Montaño, K. Liu, T. Sabo-Attwood and P. L. Ferguson, *Environ. Sci. Technol.*, 2021, **55**, 1015–1023.

27 M. J. O'Connell, S. H. Bachilo, C. B. Huffman, V. C. Moore, M. S. Strano, E. H. Haroz, K. L. Rialon, P. J. Boul, W. H. Noon, C. Kittrell, J. Ma, R. H. Hauge, R. B. Weisman and R. E. Smalley, *Science (80-.).*, 2002, **297**, 593–596.

28 S. M. Bachilo, M. S. Strano, C. Kittrell, R. H. Hauge, R. E. Smalley and R. B. Weisman, *Science (80-.).*, 2002, **298**, 2361–2366.

29 E. G. BLIGH and W. J. DYER, *Can. J. Biochem. Physiol.*, 1959, **37**, 911–917.

30 R. Wei, J. Wang, M. Su, E. Jia, S. Chen, T. Chen and Y. Ni, *Sci. Rep.*, 2018, **8**, 663.

31 K. Makide, H. Kitamura, Y. Sato, M. Okutani and J. Aoki, *Prostaglandins Other Lipid Mediat.*, 2009, 89, 135–139.

32 J. Aoki, A. Taira, Y. Takanezawa, Y. Kishi, K. Hama, T. Kishimoto, K. Mizuno, K. Saku, R. Taguchi and H. Arai, *J. Biol. Chem.*, 2002, **277**, 48737–48744.

33 T. Nakano, I. Inoue, S. Katayama, M. Seo, S. Takahashi, S. Hokari, R. Shinozaki, K. Hatayama and T. Komoda, *J. Clin. Biochem. Nutr.*, 2009, **45**, 227–234.

34 T. Nakano, I. Inoue, D. H. Alpers, Y. Akiba, S. Katayama, R. Shinozaki, J. D. Kaunitz, S. Ohshima, M. Akita, S. Takahashi, I. Koyama, M. Matsushita and T. Komoda, *Am. J. Physiol. Liver Physiol.*, 2009, **297**, G207–G214.

35 S. H. Jo, S. D. Kim, J. M. Kim, H. Y. Lee, S. Y. Lee, J. W. Shim, J. Yun, D. S. Im and Y. S. Bae, *Biochem. Biophys. Res. Commun.*, 2008, **372**, 147–151.

36 A. Grzelczyk and E. Gendaszewska-Darmach, *Biochimie*, 2013, 95, 667–679.

37 N. D. Hung, M. R. Kim and D.-E. Sok, *Lipids*, 2011, **46**, 893–906.

38 H. W. Huang, E. M. Goldberg and R. Zidovetzki, *Biochem. Biophys. Res. Commun.*, 1996, **220**, 834–838.

39 J. B. Massey, *Biochim. Biophys. Acta - Biomembr.*, 2001, **1510**, 167–184.

40 G. Beattie, C. Cohan, E. Miraflor, W. Brigode and G. P. Victorino, *Surg. (United States)*, 2019, **166**, 844–848.

41 C. Cohan, G. Beattie, W. Brigode, L. Yeung, E. Miraflor and G. P. Victorino, *J. Surg. Res.*, 2020, **245**, 604–609.

42 R. Qiao, C. Sheng, Y. Lu, Y. Zhang, H. Ren and B. Lemos, *Sci. Total Environ.*, 2019, **662**, 246–253.

43 Y. A. Hannun and L. M. Obeid, *J. Biol. Chem.*, 2002, 277, 25847–25850.

44 E. L. Johnson, S. L. Heaver, J. L. Waters, B. I. Kim, A. Bretin, A. L. Goodman, A. T. Gewirtz, T. S. Worgall and R. E. Ley, *Nat. Commun.*, 2020, **11**, 1–11.

45 E. Schwarz, S. Prabakaran, P. Whitfield, H. Major, F. M. Leweke, D. Koethe, P. McKenna and S. Bahn, *J. Proteome Res.*, 2008, **7**, 4266–4277.

46 V. Kota and H. Hama, *Adv. Biol. Regul.*, 2014, 54, 223–230.

47 J. L. Stith, F. N. Velazquez and L. M. Obeid, *J. Lipid Res.*, 2019, 60, 913–918.

48 J. M. Keriko, C. W. Chege, M. M. Magu, A. N. Murigi, M. N. Githua and Kareru, *African J. Pharm. Pharmacol.*, 2010, **4**, 745–753.

49 M. Kanehisa, Y. Sato and K. Morishima, *J. Mol. Biol.*, 2016, **428**, 726–731.

50 J. Chong, O. Soufan, C. Li, I. Caraus, S. Li, G. Bourque, D. S. Wishart and J. Xia, *Nucleic Acids Res.*, 2018, **46**, W486–W494.

51 C. Schmitz-Peiffer, *Diabetes*, 2010, 59, 2351–2353.

52 H. Ezanno, J. Le Bloc'h, E. Beauchamp, D. Lagadic-Gossmann, P. Legrand and V. Rioux, *Lipids*, 2012, **47**, 117–128.

53 M. Fu, Z. Li, T. Tan, W. Guo, N. Xie, Q. Liu, H. Zhu, X. Xie and H. Lei, *Am. J. Physiol. - Hear. Circ. Physiol.*, 2015, **308**, H11–H17.

54 J. Antonio Chavez, W. L. Holland, J. Bä, K. Sandhoff and S. A. Summers, , DOI:10.1074/jbc.M412769200.

55 J. J. DiNicolantonio and J. H. O'Keefe, *Mo. Med.*, 2017, **114**, 303–307.

56 J. A. Chavez and S. A. Summers, *Arch. Biochem. Biophys.*, 2003, **419**, 101–109.

57 T. W. Moon, *Comp. Biochem. Physiol. - B Biochem. Mol. Biol.*, 2001, 129, 243–249.

58 S. Polakof, R. Álvarez and J. L. Soengas, *Am. J. Physiol. - Regul. Integr. Comp. Physiol.*, 2010, **299**, R19–R32.

59 M. A. Caruso and M. A. Sheridan, *Gen. Comp. Endocrinol.*, 2011, 173, 227–247.

60 S. M. Adams, in *Lipids in Freshwater Ecosystems*, Springer New York, 1999, pp. 132–160.

61 A. J. Niimi and F. W. Beamish, *Can. J. Zool.*, 1974, **52**, 447–456.

62 M. Garside, *Global value of carbon nanotube market by region 2018-2026*, 2019.